Dalton Transactions

ROYAL SOCIETY OF CHEMISTRY

PAPER

View Article Online
View Journal | View Issue

Cite this: *Dalton Trans.*, 2023, **52**, 3219

Interaction of *N*-nitrosamines with binuclear copper complexes for luminescent detection†

Haosheng Feng, [a] Shao-Xiong Lennon Luo, [a] Robert G. Croy, [b] John M. Essigmann [b] and Timothy M. Swager *[a]

Received 29th November 2022,
Accepted 26th January 2023

DOI: 10.1039/d2dt03848j

rsc.li/dalton

Cu(I) from tetrakis(acetonitrile)copper(I) hexafluorophosphate ($[Cu(MeCN)_4]PF_6$) was complexed with five structurally related phosphines containing N-heterocycles. The interactions between the resulting complexes and some *N*-nitrosamines were studied using X-ray crystallography as well as emission spectroscopy. Upon complexation, three phosphine ligands bridge two Cu(I) centers to give paddlewheel type structures that displayed a range of emission wavelengths spanning the visible region. *N*-Nitrosodimethylamine (NDMA) was shown to coordinate to one of the two copper centers in some of the paddlewheel complexes in the solid state and this interaction also quenches their emissions in solution. The influence of the weakly coordinating anion on crystal and spectroscopic properties of one of the paddlewheel complexes was also examined using tetrakis(acetonitrile)copper(I) perchlorate ($[Cu(MeCN)_4]ClO_4$) as an alternative Cu(I) source. Similarly, copper(II) perchlorate hexahydrate ($Cu(ClO_4)_2{\cdot}6H_2O$) was used for complexation to observe the impact of metal oxidation state on the two aforementioned properties. Lastly, the spectroscopic properties of the complex between Ph_2P(1-Isoquinoline) and Cu(I) was shown to exhibit solvent dependence when the counterion is ClO_4^-. These Cu(I) complexes are bench stable solids and may be useful materials for developing a fluorescence based detection method for *N*-nitrosamines.

1. Introduction

N-Nitrosamines are a broad class of highly carcinogenic compounds that are activated *via* metabolism into DNA-reactive alkyl diazonium ions.[1,2] As a result, they pose a significant health risk by causing the formation of potentially mutagenic and toxic alkylated DNA bases.[3,4] They have been shown to be present in varied environments, including industrial wastes,[5–7] nitrite-preserved foods,[8,9] several pharmaceutical products,[10] and even drinking water.[11] It is important to monitor their presence in the environment with the goal of preventing exposure, but sampling is limited to selected sites and during the product manufacturing process, leaving downstream exposure unchecked. There is hence a need for novel monitoring strategies for this class of toxicants.

Current detection methods for *N*-nitrosamines have been covered recently.[1] They are often costly and time intensive, prohibiting monitoring at the consumer level. Alternative detection methods which are cheaper and less sensitive are available, but they involve chemical reactions of/with *N*-nitrosamines. Such methods require careful execution to avoid interference from breakdown products that may already be present in the sample, such as nitrite and amines. Therefore, it is highly desirable to develop a cost-effective method for direct detection of *N*-nitrosamines without the involvement of bond rearrangements.

Emission based detection methods can be highly sensitive. Unlike colorimetric measurements based on absorption which are prone to interference from ambient background light,[12] emission based methods can make use of the Stokes shift of the analyte and measurement of the emitted light can be achieved without interference from the excitation signal.

Metal complexes represent a promising platform that may respond non-destructively to *N*-nitrosamines because they can have a vacant site suitable for coordination. *N*-Nitrosamines are reported to be capable of transition metal coordination,[13] typically *via* the oxygen center.[14–16] The preferred oxygen coordination is rationalized by considering resonance structures that include a polar species with a formal negative charge at oxygen, suggesting high electron density at that site

[a]*Institute for Soldier Nanotechnologies and Department of Chemistry, Massachusetts Institute of Technology, 77 Massachusetts Avenue, Cambridge, MA, 02139, USA. E-mail: tswager@mit.edu*
[b]*Department of Chemistry, Department of Biological Engineering and Center for Environmental Health Sciences, Massachusetts Institute of Technology, 77 Massachusetts Avenue, Cambridge, Massachusetts 02139, USA*

†Electronic supplementary information (ESI) available. CCDC 2218757–2218766. For ESI and crystallographic data in CIF or other electronic format see DOI: https://doi.org/10.1039/d2dt03848j

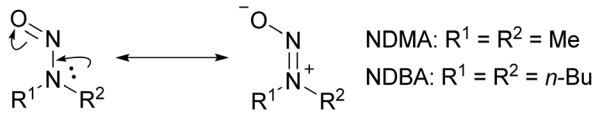

Scheme 1 Resonance structures of *N*-nitrosamines, showing the negative formal charge on oxygen. Substitutions on nitrogen for *N*-nitrosodimethylamine (NDMA) and *N*-nitrosodibutylamine (NDBA) are shown to the right.

(Scheme 1). This model is consistent with a computational study showing that the highest occupied molecular orbital (HOMO) has a significant contribution from oxygen.[17] Preceding studies on *N*-nitrosamine coordination have focused on structural characterization. However, no emission measurements on the complexes were conducted.

In addition to functioning as a binding site, emissive metal complexes are also capable of having longer lifetimes (μs) compared to those of organic molecules (ns). This is a result of the stronger spin–orbit coupling of the metal[18] that generates triplet states *via* intersystem crossing. Longer-lived species displaying phosphorescence[19] and thermally activated delayed fluorescence[20] have the ability to respond to dynamic quenching events wherein analyte diffusion to the excited species alters its electronic properties. Additionally, longer emission lifetimes can also eliminate background fluorescence in the environment through delayed signal acquisition after the excitation pulse.

Cu(I) based complexes are attractive phosphorescent materials because their fully filled 3d orbitals prevent internal quenching of excited states *via* dd transitions and hence they can be highly emissive materials.[21,22] However, these complexes generally have a preferred tetrahedral geometry in the ground state and a tendency to relax to a planar excited state geometry as a result of metal ligand charge transfer processes.[23,24] The result is that Cu(I) excited states can suffer from radiationless decay and low quantum yields. To minimize this undesired relaxation pathway of excited states, complexes must be designed with additional rigidity by appropriate choice of ligands.[20] Multiple reviews have been written on luminescent Cu(I) complexes, covering topics such as their photophysical[22,25] and structural properties[26] as well as potential applications.[27]

One way of introducing rigidity into Cu(I) complexes is to use binuclear structures. Bidentate ligands containing P and N can create a rigid network that bind Cu(I) salts with weakly coordinating anions such as BF_4^- or PF_6^- in paddlewheel type complexes. In the case of phosphine **1** (Fig. 1), not only has the Cu(I) complex been shown to be competent of accepting several solvent molecules as ligands,[28] but these materials also exhibit different photophysical parameters in the solid state. Structurally similar Ag(I) complexes[29] have also been shown to have nitrile ligands that may be easily exchanged for other organic nitriles. This suggests that these and related complexes may be capable of differentiating between different coordinating analytes, including *N*-nitrosamines. The phenomenon of ancillary ligands affecting emission properties of Cu(I) complexes has been limited to only few previous investigations.[30,31]

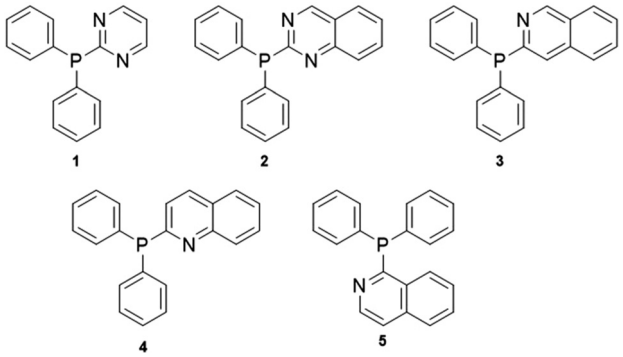

Fig. 1 N-heterocyclic phosphines synthesized and examined for complexation with Cu(I) in this study. **1**: Ph_2P(2-pyrimidine); **2**: Ph_2P(2-quinazoline); **3**: Ph_2P(3-isoquinoline); **4**: Ph_2P(2-quinoline) and **5**: Ph_2P(1-isoquinoline).

We have been interested to determine if suitable Cu(I) paddlewheel complexes could be used for *N*-nitrosamine sensing. To this end we synthesized a series of structurally related phosphines containing different extended N-heterocycles in addition to the previously reported phosphines **1** and **5** (Fig. 1).[28,32] We examined a series of Cu(I) complexes and how their emission properties can be tuned. Electronic and steric differences caused the complexes to have different affinities for *N*-nitrosamines and we have sought to elucidate factors that govern their *N*-nitrosamines affinity. The effect of weakly coordinating anions and metal oxidation state was also investigated using phosphine **5**.

2. Results and discussion

Copper complexes of phosphines **1–5** were synthesized using $[Cu(MeCN)_4]PF_6$ as the Cu(I) source to give compounds **1-Cu** to **4-Cu** and **5-Cu-PF$_6$**. The influence of counterion was investigated by also using $[Cu(MeCN)_4]ClO_4$ as an alternative source of copper(I) when forming a complex with phosphine **5** to give **5-Cu-ClO$_4$**. Copper(II) perchlorate was also complexed with phosphine **5** to examine the role of oxidation state in the overall structure of **5-Cu-II**.

2.1 Structural characterizations

2.1.1 General description of crystal structures. Crystals suitable for X-ray crystallography studies were grown using copper complexes of phosphines **1–5**. All successfully crystallized copper(I) complexes adopted paddlewheel structures with two copper centers flanked by three bidentate phosphine ligands, each chelating through phosphorus and one nitrogen. Due to the asymmetry of the ligand, the overall structure of the complex may adopt two different linkage isomers (Fig. 2).[33] If a copper atom is coordinated by either three phosphorus or nitrogen atoms, this is termed head-to-head (HH) isomer. The

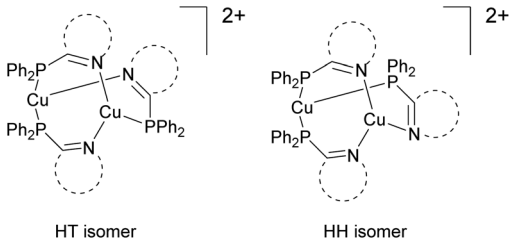

Fig. 2 Two possible structures are possible for the binuclear complexes depending on the orientation of the three ligands. Left: head-to-tail (HT) isomer and right: head-to-head (HH) isomer.

alternate isomer, where one of the three ligands is flipped and each copper has either two phosphorus and one nitrogen atom or the inverse, is called head-to-tail (HT).

Most of the obtained structures crystallized exclusively as one of the two isomers, except for **3-Cu** which crystallized as a mixture of the two linkage isomers (2.1.4). One of copper ions is usually four coordinate with an additional solvent ligand assembled during crystallization, and the other copper remains three coordinate. For the HH structures, the ligand is usually acetonitrile, which binds to the copper ion bound to phosphorus.

Consistent with the resonance form of *N*-nitrosamines, they have a 3-center-4-electron π system and are capable of π type interactions in addition to being a σ donor. As a result of their polar structure, we expected them to be strong σ donor type ligands that could outcompete solvent for coordination to the copper centers. Upon crystallizing from solution in the presence of *N*-nitrosodimethylamine (NDMA), the solvent ligands are displaced in some complexes (Fig. 3e and f).

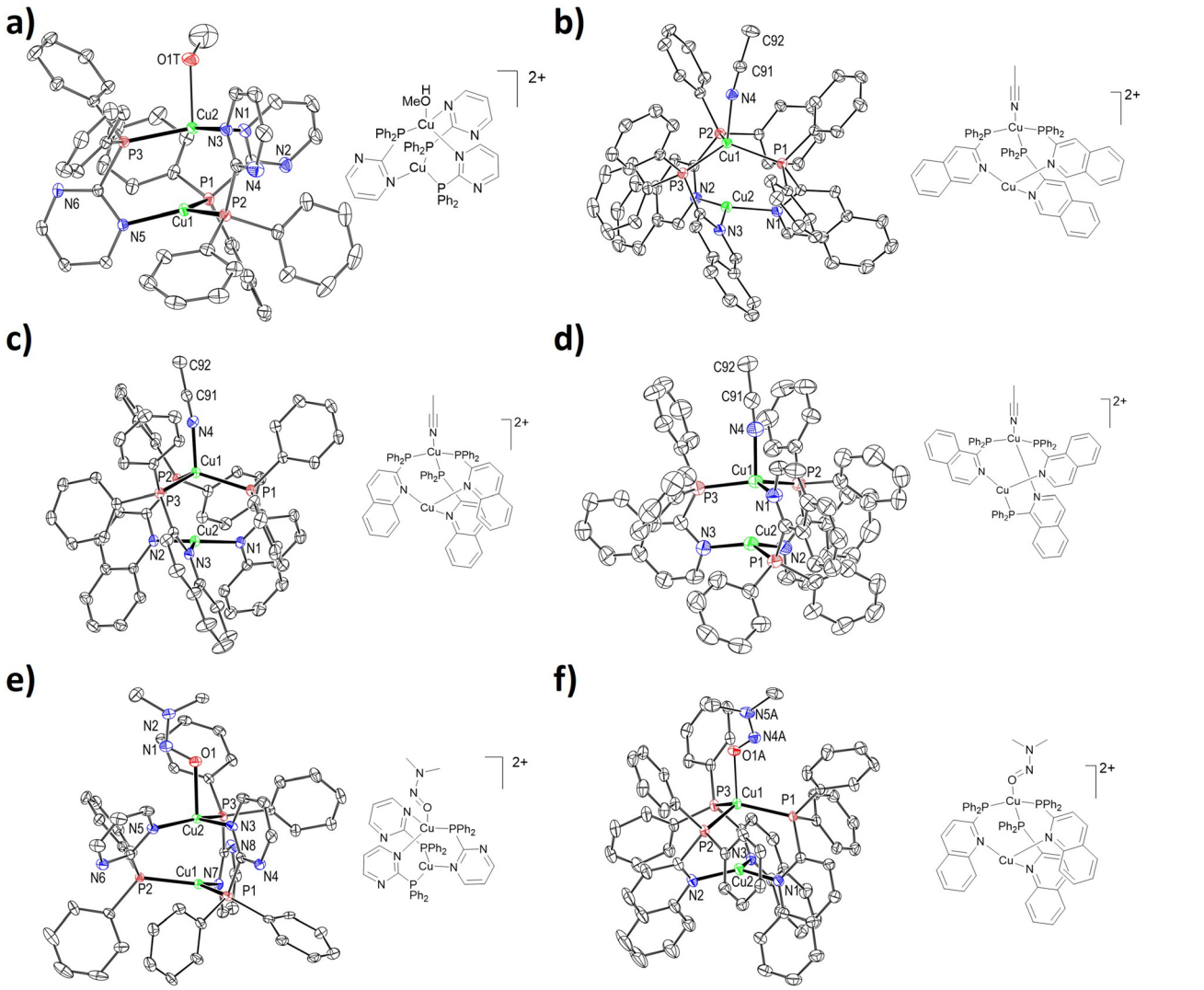

Fig. 3 Thermal ellipsoid plots of several dinuclear Cu(I) complexes obtained at the 50% probability level alongside their respective schematic representations. (a) **1-Cu**, (b) major isomer of **3-Cu**, (c) **4-Cu**, (d) **5-Cu-ClO$_4$**, (e) **1-Cu-NDMA** and (f) **4-Cu-NDMA**. Hydrogen atoms, counterions (PF_6^-, ClO_4^-), solvent molecules and disordered portions have been omitted for clarity. For more detailed information on crystallography data, please refer to the ESI.†

2.1.2 Ph_2P(2-Pyrimidine) 1-Cu. In the crystal structure, MeOH binds to Cu2 that is complexed by two nitrogen-based ligands (Fig. 3a). This selectivity may be the result of Cu2 being more sterically accessible, with fewer surrounding phenyl groups than the phosphine rich Cu1. Furthermore, Cu2 may be considered electronically harder than Cu1 that is complexed to two more polarizable phosphorus ligands. The oxygen on MeOH, which lacks any resonance delocalization is a hard ligand. When NDMA was present during crystallization, it displaced MeOH at Cu2 to give **1-Cu-NDMA** (Fig. 3e). Compared to solid NDMA at 130 K,[34] the NDMA in **1-Cu-NDMA** at 100 K has a lengthened O1–N1 distance of 1.274(5) Å rather than 1.260(6) Å and a shortened N1–N2 distance of 1.301(5) Å rather than 1.320(6) Å. The data from these two crystals reflect an increased contribution from the polar resonance structure of NDMA upon coordinating to Cu2. The N1–O1–Cu2 angle was determined to be 118.2(2)°, so the N2–N1–O1 π system is not significantly involved in bonding and *N*-nitrosamines act more as σ-donors rather than π-acceptors.

The Cu–O bond distance has a value of 2.194(3) Å, smaller than the sum of van der Waal radii[35] of Cu^+ and O, which are 1.73 and 1.71 Å respectively. This distance is however longer than that predicted for a Cu–O single bond[36] at 1.75 Å. Taken together, this suggests that the interaction is weak. This may be intuitively rationalized since Cu^+ has a filled valence shell and the higher energy vacant 4s and 4p orbitals may lack sufficient bonding interactions to the oxygen.

2.1.3 Ph_2P(2-quinazoline) 2-Cu. Unfortunately, after extensive attempts, only polycrystalline material was obtained and no single crystals suitable for crystallographic analysis were isolated. This may be due to the two inequivalent nitrogens on phosphine **2** having similar affinities to copper, making multiple ligand arrangements possible. Thus, a complex mixture of isomers in solution prevents the growth of an ordered single crystal.

X-ray photoelectron spectroscopy (XPS) results showed that the measured atomic ratios closely match the expected values based on a binuclear structure (Table 1), similar to the other Cu(I) complexes reported herein. The lower than expected value for N might be attributed to some loss of the MeCN ligand under the ultra-high vacuum conditions during data collection. The N 1s spectrum can be deconvoluted into three signals representing uncoordinated and coordinated quinazoline nitrogens[37] as well as acetonitrile[38] (Fig. S60c†) while the two peaks in the P 2p spectrum are assigned to coordinated phosphines[39] as well as PF_6^- anions[40] (Fig. S60e†). No oxidation of Cu(I) was observed based on the absence of Cu(II) satellite peaks (Fig. S60f†).[41] Together with high resolution mass spectrometry data showing reasonable fragments of a binuclear structure (4.3.2), we think that it is highly likely for **2-Cu** to adopt such a structure in the solid state in the absence of a crystal structure. The single ^{31}P NMR signal (Fig. S25†) may be consistent with a postulated HH structure (Fig. S60a†).

Table 1 XPS results on atomic ratios for a sample of **2-Cu** assuming a binuclear structure with two Cu(I) centers, three ligands and two counterions

	C	Cu	F	N	P
Molecular formula	62	2	12	7	5
Expected atomic ratio (%)	70.45	2.27	13.63	7.95	5.68
Measured atomic ratio (%)	71.45	2.32	13.83	6.62	5.78

2.1.4 Ph_2P(3-isoquinoline) 3-Cu. The complexes crystallized as a mixture of HH (Fig. 3b) and HT isomers. Fitting of the X-ray diffraction data suggested that the HH structure was dominant at approximately 93%. Not only may the extended isoquinoline ring have an intrinsic preference for one geometry over the other, but crystallization conditions such as solvent[33] and temperature can also influence the geometry as well, convoluting analysis.

MeCN served as the ligand to the phosphorus rich Cu1 in both the HT and HH isomers. Cu(I) is classified as soft according to hard–soft acid base concepts,[42,43] hence it may have stronger interactions with soft phosphorus, resulting in a more electron rich center compared to the other copper site. The Cu–N bond distance (1.142(3) Å) is comparable to values reported in literature for structurally similar complexes.[44] The MeCN molecule also does not interact with Cu1 head on, instead making a Cu1–N4–C91 angle of 165.89(16)°. This deviation from linearity has been observed in other coordination compounds involving Cu(I) and MeCN.[45,46] The MeCN molecular fragment remains largely linear with a N4–C91–C92 angle of 178.5(2)°, suggesting that there is no significant back bonding from Cu1. MeCN was not displaced when **3-Cu** was crystallized in the presence of NDMA. Crystals under this condition retain MeCN coordination to the phosphorous rich Cu1, although the overall refinement quality of the structure was reduced (Fig. S58, and Table S1†).

2.1.5 Ph_2P(2-quinoline) 4-Cu. The HH geometry was isolated by crystallization and MeCN coordinated to phosphorous rich Cu1 (Fig. 3c), consistent with observations for **3-Cu** and **5-Cu-ClO_4**. The Cu1–N4–C91 and N4–C91–C92 angles of the MeCN were 166.02(17) and 178.3(2)° respectively, similar to those in **3-Cu**. MeCN was partially displaced when **4-Cu** was crystallized with NDMA present to give **4-Cu-NDMA** (Fig. 3f), with a ratio of approximately 8 : 2 MeCN : NDMA in the final refined structure. The NDMA complexation was promoted by using non-coordinating DCM as the crystallizing solvent. The geometry of binding again suggests that NDMA is acting as a σ donor, with a N4A–O1A–Cu1 angle of 123.4(14)°.

2.1.6 Ph_2P(1-isoquinoline) 5-Cu-ClO_4. This complex adopted the HT geometry and MeCN coordinated to the phosphorous rich Cu1 (Fig. 3d). Unexpectedly, the MeCN was displaced by ClO_4^- when **5-Cu-ClO_4** was crystallized in the presence of NDMA. The resulting crystal also had a reduced refinement quality (Fig. S59, and Table S1†), similar to what was observed when crystallizing **3-Cu** together with NDMA.

2.1.7 5-Cu-II. When $Cu(ClO_4)_2{\cdot}6H_2O$ was used as the copper source to complex phosphine **5**, the resulting product **5-Cu-II** gave blue crystals upon crystallization from MeCN–Et_2O. Initial electron paramagnetic resonance (EPR) measure-

ments displayed an axial signal[47,48] (where the g tensor has values of $g_x = g_y \neq g_z$) while **5-Cu-ClO$_4$** was EPR silent (Fig. S68†), indicating the preservation of Cu(II). This was further supported by a Cu : Cl ratio of 1 : 2 in the empirical formula determined from X-ray diffraction, which revealed a structure with a single copper center surrounded by two ligands (Fig. 4) rather than a paddlewheel structure. Interestingly, the phosphorus centers were oxidized from phosphines to their corresponding phosphine oxides.

The copper adopts a pseudo square planar geometry as is common for Cu(II) complexes, with a O1–N1–O2–N2 torsion of 14.24(6)°. As both Cu(II) and ClO_4^- exhibit oxidative properties,[49,50] either of the two species could have been responsible for the oxidation of P(III) to P(V). However, Cu(II) is the more likely oxidant on account of the stability of product when using $[Cu(MeCN)_4]ClO_4$ as a Cu(I) source as well as prior literature describing oxidation of phosphines by Cu(II).[51] As the complexation reaction was carried out under air using $Cu(ClO_4)_2{\cdot}6H_2O$ as the metal precursor, either water or molecular oxygen could have served as the oxygen source. To investigate this, we assembled **5-Cu-II** from **5**'s phosphine oxide (**5-O**) and repeated our original synthesis from **5** under degassed conditions (Scheme 2). The product from the degassed reaction did not exhibit the broad ^{1}H NMR signals attributable to **5-Cu-II** (Fig. S47†), suggesting that molecular oxygen was required for the oxidation of **5** under our reaction conditions. When NDMA was present during crystallization, it was not incorporated into the structure (Fig. S57†).

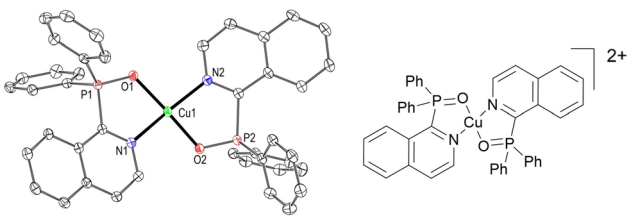

Fig. 4 Thermal ellipsoid plot of **5-Cu-II** at 50% probability alongside its schematic representation. Hydrogens and counterions are omitted for clarity.

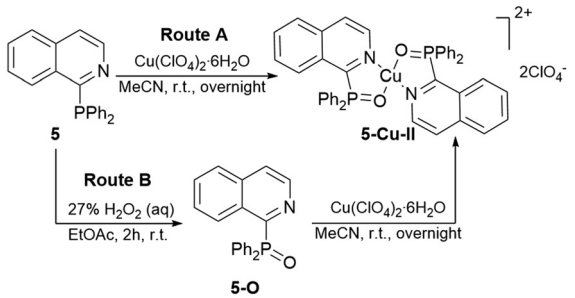

Scheme 2 Two synthetic routes towards **5-Cu-II**. Route A: directly from phosphine **5**. Route B: oxidation of **5** to its oxide **5-O** before its complexation with Cu(II).

This structural motif is consistent with previous reports by Trigulova *et al.*[52,53] who assembled structurally similar complexes directly from phosphine oxides. They could also obtain the Cu(II) complexes *via* the aerobic oxidation of Cu(I) and its coordinated phosphines during crystallization. In contrast, all obtained complexes with Cu(I) salts presented here were air stable as solids (several months) and in solution over the time span of crystallization (approximately 3 days), suggesting that the aryl rings on phosphine and/or the lower strain in an acyclic phosphine lowers its propensity as well as that of Cu(I) towards aerobic oxidation.

2.2 Spectroscopic measurements

Some of the free phosphine ligands have been previous reported in literature[23,32] and their absorption spectra generally display broad features consistent with what was observed here (Fig. 5). Measurements were conducted in chloroform ($CHCl_3$) solution under ambient conditions, except for **4** and **4-Cu** due to poor solubility of the latter in chloroform. Acetonitrile (MeCN) was used to dissolve these two compounds for characterization to maintain consistency. We used $CHCl_3$ as much as possible in order to minimize disrupting the binuclear structure in solution, as comparing the NMR spectra of **5-Cu-PF$_6$** in CD_3CN and $CDCl_3$ suggests that the more coordinating acetonitrile breaks up the binuclear structure (Fig. S35, and S36†).

We verified that phosphine **5** did not undergo significant oxidation during emission measurements by synthesizing its oxide **5-O** and characterizing its emission under the same experimental conditions. While both **5** and **5-O** has an emission around 420 nm which may indicate the presence of some oxidized phosphine, it is only a minor component in **5**'s emission spectrum (Fig. S61†). Extrapolating this to the other phos-

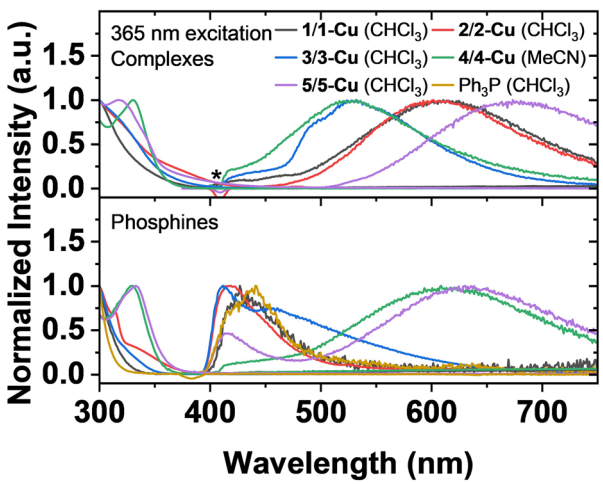

Fig. 5 Absorption and emission (λ_{ex} = 365 nm) measurements on Cu(I) complexes (top) and phosphines (bottom) in solution. PPh_3 was used as a reference for phosphines and not used during complexation. Data was individually normalized relative to the maximum intensity value of each trace. The asterisk (*) at 410 nm indicates where the Raman scattering from residual water was before background subtraction.

phines examined herein suggests that their main emission component measured should originate from their unoxidized forms rather than their oxides.

Phosphine **1** has similar absorption and emission characteristics to that of triphenylphosphine (Ph_3P), suggesting that its electronic structure is not significantly perturbed by the pyrimidine substituent. Phosphines **2**, **4** and **5** had a local maxima at 314, 330 and 333 nm respectively, while **1** and **3** had monotonically increasing absorbance spectra with no local maxima going from 400 down to 300 nm. Complexation with Cu(I) produces a red shift in the absorption spectra and a shoulder develops towards the lower energy region, which is pronounced for complexes **2-Cu**, **3-Cu** and **5-Cu-PF$_6$**. This feature may be attributed to a charge transfer process between the Cu center and ligands, which has been reported upon in literature for Cu(I) based complexes.[28,54] The complexes had molar absorption coefficients (ε) at 275 nm between 1.5–5.4 × 10^4 M^{-1} cm^{-1} (Fig. S69a†), with the complexes bearing ligands **2–5** having higher values and **1-Cu** having the lowest values, likely due to the lower π conjugation in pyrimidine compared to the other N-heterocycles. ε values at other selected wavelengths are provided in Table 2.

2.2.1 Emission spectra in solution. The Cu(I) complexes of phosphines **1–5** display a range of emission colors in the visible region, varying from green to red. This variation is attributed to the increased conjugation afforded by the appended aryl ring for phosphines **2–5** compared to phosphine **1**, as well as different electronic character of the heteroaromatic rings depending on the substitution patterns. In solution, all copper complexes were only weakly emissive, consistent with previous reports on Cu(I) based complexes.[23] Possible quenching pathways invoked in the literature include solvent interaction[55] as well as exciplex formation.[56] To obtain their solution phase measurements, we used a concentration of 150 μM and at these high concentrations the quantum yield measurements are unreliable as a result of inner filter effects.[57] However, we infer that the quantum yields are less than 1% based on the low signal to noise ratio of acquired data.

When analyzing steady state measurements, the Raman scattering peak from residual water present in the solvent was removed by performing background subtraction using a solvent-only sample as reference. The emission spectra of the examined compounds were largely broad, consistent with a charge transfer emission pathway reported for similar compound classes (Fig. 5).[23] **1-Cu**, **2-Cu**, **4-Cu** and **5-Cu-PF$_6$** have single emission maxima at 610, 605, 530 and 675 nm respectively, while **3-Cu** emits primarily at 530 with a slight shoulder at 495 nm. **5-Cu-PF$_6$** has the longest emission wavelength and can be compared to **3-Cu**, which is its structural isomer. The smaller degree of red shift when using **3** compared to **5** during complexation has been observed in structurally similar complexes in literature and was attributed to the phosphino substituent in the 1-position stabilizing the lowest unoccupied molecular orbital (LUMO) of isoquinoline more than when it is in the 3-position.[23]

2.2.2 Comparison with solid phase emission spectra. Solid phase emissions of the Cu(I) complexes were acquired after dropcasting their solution onto a quartz cover slip and removing the solvent *in vacuo*. To ensure that the vacuum exposure did not result in significant loss of the coordinated ligands, we characterized **5-Cu-PF$_6$** directly as a powder and compared its emission to that of material dropcast and dried *in vacuo*. ^{1}H NMR on a sample of the powder suggests that MeCN is present as the ligand based on the chemical shift at 1.72 ppm (Fig. S62†). Furthermore, its 1 : 1 integration ratio to the signal at 9.3 ppm indicates that every complex has a bound ligand as each binuclear complex has three P^N ligands.

Fig. S63† shows that the emission spectra of the vacuum treated material is identical to that of the powder, strongly suggesting that the MeCN ligand remains bound under short vacuum exposure. Likewise, we expect this to be the same for other examined complexes.

In the solid phase, 3 of the 5 complexes had their emission spectra blue shifted when compared to in solution while retaining their broad features (Fig. 6). **1-Cu**'s emission peak shifted from 610 nm in solution to 513 nm in the solid state, **2-Cu**'s shifted from 605 to 585 nm, and **5-Cu-PF$_6$**'s shifted from 675 to 640 nm. This phenomenon may be attributed to solvent relaxation effects[58] that typically reduce the energy gap

Table 2 Extinction coefficients of reported compounds in chloroform/acetonitrile solution at selected wavelengths

Compound	Solvent	λ (nm)	ε (M^{-1} cm^{-1})
1-Cu	$CHCl_3$	297	14 323
2-Cu	$CHCl_3$	321	19 615
		372	5347
3-Cu	$CHCl_3$	281	53 122
		325	30 988
4-Cu	MeCN	264	61 849
		317	20 082
		330	24 720
5-Cu-PF$_6$	$CHCl_3$	279	37 069
		318	33 979
		333	22 843
5-Cu-PF$_6$	MeCN	275	26 002
		331	16 891
5-Cu-ClO$_4$	$CHCl_3$	279	38 163
		316	28 927
		333	21 976
5-Cu-ClO$_4$	MeCN	275	26 725
		331	17 327
5-Cu-II	MeCN	279	10 416
		329	9349
		345	5817
5	$CHCl_3$	279	9134
		333	5607
5	MeCN	279	8531
		333	5515

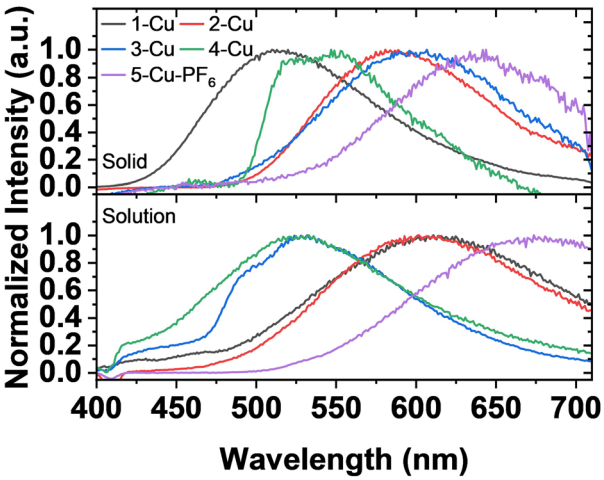

Fig. 6 Comparing the emission spectra (λ_{ex} = 365 nm) of complexes **1–4-Cu** and **5-Cu-PF$_6$** as solids (top) and in solution (bottom). Solvents used for solution phase measurements may be found in Fig. 5.

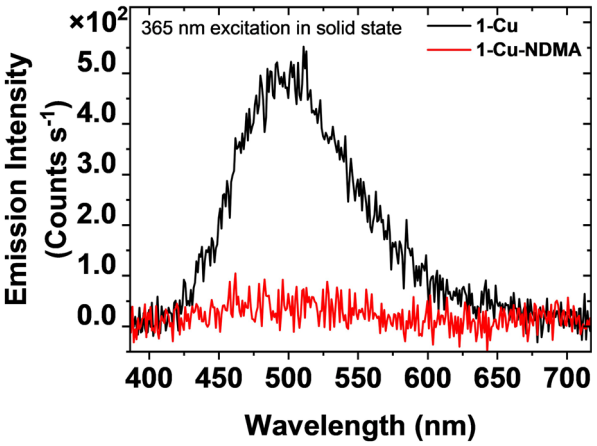

Fig. 7 Solid state emission spectrum (λ_{ex} = 365 nm) of **1-Cu** when recrystallized from (a) DCM/MeOH in the absence of NDMA (black trace) and (b) DCM/Hexanes in the presence of NDMA (red trace). The latter complex is much less emissive.

between the excited state's ground vibrational level and the ground state. Since this non radiative relaxation pathway is inaccessible in the solid phase, a larger energy gap between excited and ground states is maintained and results in higher energy emissions.

In contrast, **3-Cu**'s emission profile became less defined and displayed a red shift in the solid phase. It now has a single peak at 600 nm instead of the two peaks in solution. Although the crystal structure suggests the presence of both HH (93%) and HT (7%) species in the solid state and both can therefore contribution to the emission signal, the contribution from the HH isomer should dominate in this case. Lastly, **4-Cu**'s solid emission profile is narrower and more defined than that in solution. It now displays two peaks at 525 and 550 nm as opposed to its single peak at 530 nm in solution. These observations for **3-Cu** and **4-Cu** suggest that the complexes may not retain their solid phase structures in solution.

2.2.3 Interaction with *N*-nitrosamines. On addition of different equivalents of NDBA from a stock solution, the solution emission of **1-Cu** was quenched while retaining its general spectral shape, with higher amounts of NDBA resulting in more quenching (Fig. S64†). Similar to a previous literature report,[28] the methanol coordinated complex was highly emissive in crystallized form (Fig. 7). It showed a broad emission spectrum with the highest intensity at approximately 500 nm and had an estimated photoluminescent quantum yield (PLQY) of 28%. The NDMA complexed material displays an emission profile with the same general shape but is largely quenched, giving a PLQY value of 5.5%.

The same trend of increased emission quenching with increasing amounts of NDBA was also observed for **2-Cu**, **4-Cu** and **5-Cu-PF$_6$** (Fig. S64†). We also performed a preliminary selectivity study for **5-Cu-PF$_6$** using NDBA, NDMA as well as dibutylamine (DBA). We prepared stock solutions of the three analytes in chloroform before adding different amounts to

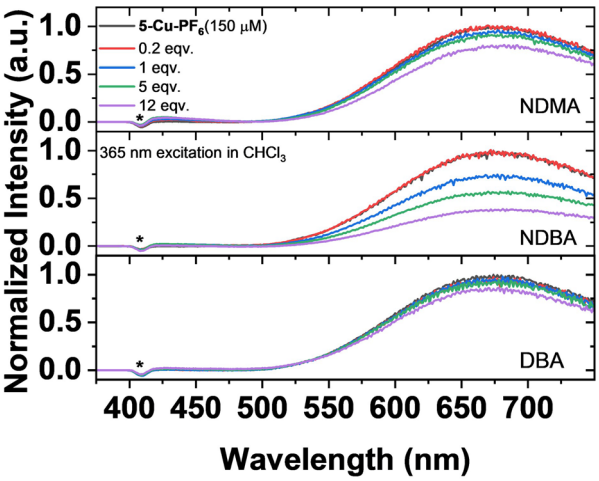

Fig. 8 Response of **5-Cu-PF$_6$** to various equivalents of NDMA (top), NDBA (middle) and DBA (bottom) in chloroform solution (λ_{ex} = 365 nm). Different degrees of quenching were measured for each analyte. Data for each analyte is normalized relative to the trace when no analyte was present. The asterisk (*) at 410 nm indicates where the Raman scattering from residual water was before background subtraction.

chloroform solutions of **5-Cu-PF$_6$**. The results suggest that among the three compounds, NDBA is the best emission quencher, followed by NDMA and lastly DBA (Fig. 8). Since NDBA's quenching ability is larger than the sum of that for NDMA and DBA, it is possible that the nitroso group has a synergistic effect together with the longer alkyl chains. DBA was also compared to NDBA using **4-Cu** (Fig. S65†) in acetonitrile solution and DBA barely quenched its emission compared to NDBA. This suggests that the nitroso group plays an important role as an effective quencher of this class of dinuclear copper complexes. It is notable that although *N*-nitrosamines can undergo photofragmentation and create

reactive species upon radiation at 365 nm,[1] no significant changes in emission spectra were observed during the quenching studies. This suggests that the Cu(I) complexes are photochemically stable in the presence of *N*-nitrosamines.

In contrast with the rest of the aforementioned complexes, **3-Cu** shows an unusual trend with increasing amounts of NDBA. Its emission profile actually increased in intensity between 0 and 1 equivalent of NDBA. When 2–12 equivalents of NDBA were introduced, the emission spectra first reaches an intensity plateau at 2 equivalents before getting quenched between 4 and 12 equivalents (Fig. 9, and Fig. S66†). This unexpected increase in emission intensity up to a 1 : 1 (**3-Cu** : NDBA) stoichiometry suggests that the complex undergoes a structural change upon irradiation in the presence of NDBA, possibly due to reaction with the NDBA fragmentation products. At super stoichiometric amounts of NDBA, an additional collisional quenching mechanism likely dominates.

As we observe emission quenching for complexes that did not crystallize with NDMA, it appears that the binding interaction between the NDMA oxygen and copper is rather weak. The interaction of NDMA was also investigated by NMR for **5-Cu-ClO$_4$** (Fig. S41 and S42†) and **5-Cu-II** (Fig. S46†) and both did not show significant changes in chemical shifts upon NDMA introduction. Therefore, the observed emission quenching in solution is likely a result of collisions between NDBA and the excited complexes rather than the formation of a static NDBA–Cu complex.

2.2.4 Quantifying emission responses to NDBA. We performed fluorescence titration measurements on **1-Cu**–**4-Cu** as well as **5-Cu-PF$_6$** and **5-Cu-ClO$_4$** to assess their potential for detection of NDBA. Using the same NDBA sample for each of the five Cu(I) complexes, we added increasing amounts of NDBA to the solutions and tracked their changes in emission spectra at 610, 605, 530, 530 and 675 nm respectively. Except for **3-Cu**, all other complexes had their emission quenched by NDBA. We therefore performed linear fitting over the range of NDBA equivalents added to obtained Stern–Volmer constants (K_{SV}) of 0.146, 0.0562, 0.0600, 0.127 and 0.0757 respectively (Fig. S67†).

Due to its unusual response to NDBA among the complexes examined, more data points were collected for **3-Cu**, which had a linear response towards NDBA between 0 and 1 equivalent (Fig. 9). Fitting of the data and solving for the amount of NDBA that would give a normalized emission intensity value (F_0/F) corresponding to three times the standard deviation[59,60] from the emission intensity at 0 equivalents NDBA (F_0) gave a limit of detection value at 0.12 equivalents, or 2.8 ppm (18 μM) at the complex concentration used (150 μM) for titration (Fig. S66†).

2.2.5 Role of anion and solvent in 5-Cu. Both **5-Cu-PF$_6$** and **5-Cu-ClO$_4$** share similar features in their absorption spectra in both chloroform (Fig. 10a) and acetonitrile (Fig. 10b). However, their absorptions in MeCN more closely resemble that of free phosphine **5** which suggests that the more coordinating MeCN may be fragmenting the binuclear structure. This is supported by their lower ε values in MeCN compared to in $CHCl_3$ (Fig. S69b,† and Table 2). In $CHCl_3$, the complexes' absorption spectra display a blue shifted maxima (from 333 to 316 nm) and a shoulder around 380 nm when compared to **5**. Fig. 10c and d shows the same absorption spectra classified by anion rather than by solvent, illustrating that **5** exhibits less solvatochromism when compared to **5-Cu-PF$_6$** and **5-Cu-ClO$_4$**.

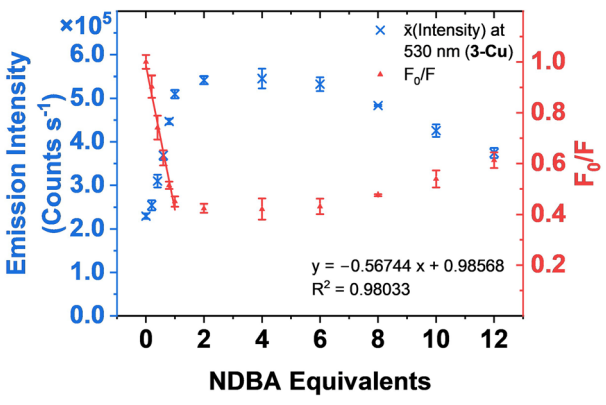

Fig. 9 Stern–Volmer analysis performed on **3-Cu** when adding increasing amounts of NDBA to the same sample. F_0 = normalized emission intensity at 0 equivalents NDBA. $\bar{x}$ = mean emission intensity value. Error bars represent one standard deviation from the mean.

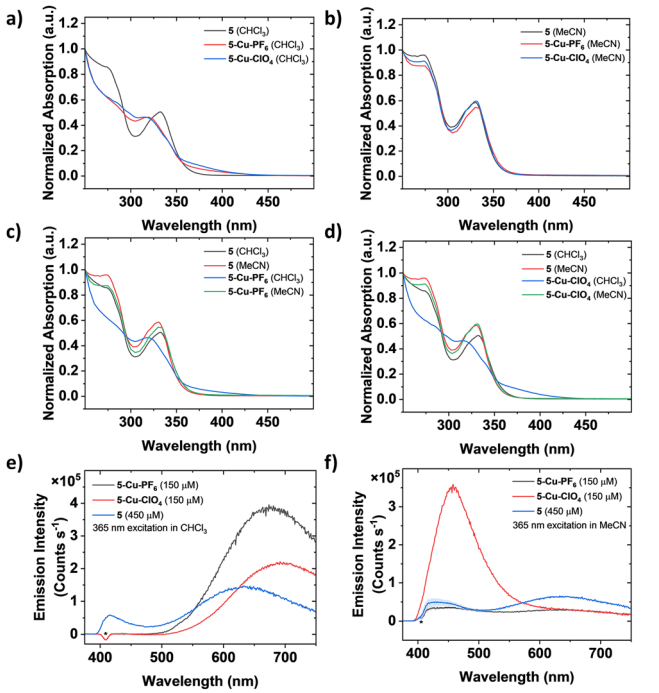

Fig. 10 Absorption spectra of **5**, **5-Cu-PF$_6$** and **5-Cu-ClO$_4$** between 250 and 500 nm classified by solvent (a and b) and anion (c and d). Each spectrum was normalized to its highest absorbance value. (e and f) Emission spectra showing the concentration of **5**, **5-Cu-PF$_6$** and **5-Cu-ClO$_4$** used, classified by solvent. The asterisk (*) at 410 nm indicates where the Raman scattering signal of residual water was before background subtraction.

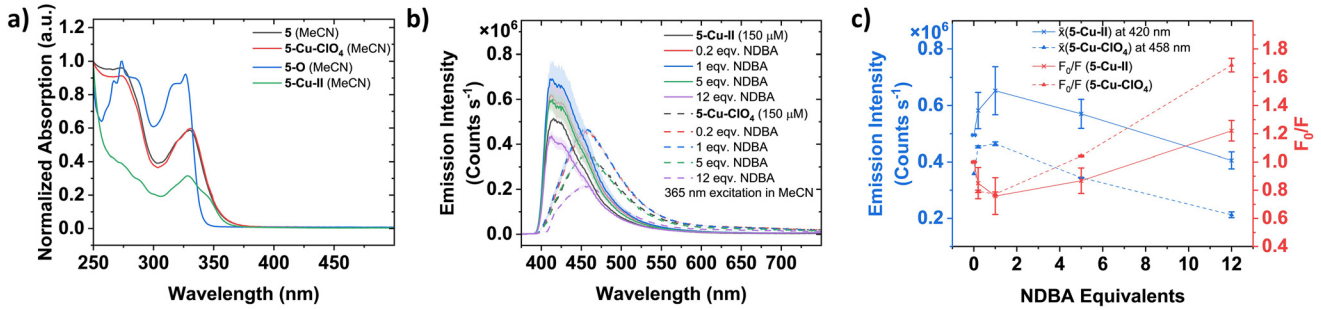

Fig. 11 (a) Absorption spectra of **5**, **5-Cu-ClO$_4$** and **5-Cu-II** in MeCN between 250 and 500 nm, normalized to each spectra's highest absorbance value. (b) Emission spectra (λ_{ex} = 365 nm) of **5-Cu-ClO$_4$** and **5-Cu-II** in MeCN solution when exposed to increasing equivalents of NDBA. (c) Stern–Volmer analysis on **5-Cu-ClO$_4$** and **5-Cu-II** using different equivalents of NDBA. F_0 = normalized emission intensity at 0 equivalents NDBA. $\bar{x}$ = mean emission intensity value. Shaded region in emission spectra represents one standard deviation from $\bar{x}$.

In the emission spectra, **5-Cu-ClO$_4$** has a similar spectral shape to **5-Cu-PF$_6$**, although the former is less emissive in $CHCl_3$ (Fig. 10e) and has a slightly redshifted emission maximum (695 compared to 675 nm). In MeCN, the trend is reversed with the emission of **5-Cu-PF$_6$** essentially absent whereas **5-Cu-ClO$_4$** has a prominent emission at 458 nm (Fig. 10f). Comparisons with the emission of phosphine **5** in the two solvents demonstrate free phosphine is not present in significant amounts in solutions of **5-Cu-PF$_6$** and **5-Cu-ClO$_4$**. Therefore, the anion appears to primarily affect the excited state rather than the ground state of the cationic core. It is possible that similar effects may be observed for the other phosphine ligands (**1–4**) when switching between weakly coordinating anions.

2.2.6 Role of Cu(II) when complexing with 5. Substituting $Cu(ClO_4)_2{\cdot}6H_2O$ for $[Cu(MeCN)_4]ClO_4$ as the copper source gave **5-Cu-II** which has a markedly different absorption profile compared to **5-Cu-ClO$_4$** (Fig. 11a). This is consistent with the Cu(II) complex having a different structure compared to its Cu(I) analogue as illustrated earlier (2.1.7) since **5-Cu-II** adopts a square planar geometry and its ligands are now phosphine oxides. Compared to **5-O**, **5-Cu-II** has a shoulder in its absorption spectra at 365 nm as well as fewer fine features overall.

We were initially puzzled that luminescence measurements on **5-Cu-II** gave a detectable signal as Cu(II) ions are often used as quenching agents.[61–63] However, there is some literature precedence for luminescent complexes bearing Cu(II) where the ligands are porphyrins[64–66] and salens.[67] To ensure that our observed emission did not come from impurities, as well as to remove potential side reactions during our initial attempt of oxidizing phosphine **5** in presence of $Cu(ClO_4)_2{\cdot}6H_2O$, we assembled **5-Cu-II** using an alternate route (Scheme 2). As outlined in route (B), we first oxidised phosphine **5** to its phosphine oxide **5-O**. $Cu(ClO_4)_2{\cdot}6H_2O$ was then used to introduce Cu(II) for complexation. Compared to route (A), the resulting material from route (B) gave a cleaner ^{1}H spectrum without the sharp peaks between 7.5 and 8.6 ppm while maintaining the broad features likely due to the paramagnetic nature of the complex (Fig. S47†). No ^{31}P signals were observed for material obtained *via* route (B), while a signal at −6.9 ppm was measured for material obtained from route (A). These extraneous signals do not match those from either **5** or **5-O** and may hence represent intermediate species during phosphine oxidation.

Nonetheless, **5-Cu-II** synthesized from route (B) still displayed luminescence in acetonitrile solution. At first glance, one possible origin for this emission may be uncoordinated **5-O**, given that the normalized emission spectra of **5-Cu-II** and **5-O** are highly similar (Fig. S70a and S70b†). However, the pre-normalization data indicates that even at triple the concentration, **5-O** has a lower emission intensity in MeCN compared to **5-Cu-II**. Furthermore, the lack of a ^{31}P signal after extended data acquisition indicates that the ligand interacts strongly with Cu(II) and no free ligands are present in solution. The excitation spectra of **5-O** and **5-Cu-II** are also different, suggesting that **5-Cu-II** has a distinct excited state (Fig. S70c and S70d†). Hence, we believe that the complex itself is the most likely source of emission.

5-Cu-II also displayed a more intense emission in MeCN compared to **5-Cu-ClO$_4$** and showed a slightly blue shifted maximum at 430 rather than 458 nm (Fig. 11b), even though **5-Cu-II** had the lowest molar absorption coefficients (Fig. S69b†, Table 2). We were not able to produce crystal structures with NDMA, however **5-Cu-II** was more sensitive to NDBA addition than **5-Cu-ClO$_4$**. Similar to **3-Cu**, both **5-Cu-ClO$_4$** and **5-Cu-II** demonstrated increasing emission intensity up to one equivalent of NDBA before undergoing quenching at higher equivalents (Fig. 11b and c).

3. Conclusions

A series of bidentate heterocyclic phosphine compounds and their corresponding Cu(I) complexes were synthesized. Their interactions with two *N*-nitrosamines were then examined in solution and in the solid state for **1-Cu**. In stoichiometric excess, *N*-nitrosamines were found to be emission quenchers in solution, possibly *via* a collisional pathway. Crystalline NDMA complexes were prepared for some of the Cu(I) complexes, wherein the *N*-nitrosamine displaces a coordinated

solvent molecule. When coordinated to copper, NDMA displayed bond lengths resembling more of its polar resonance form. In solution, some Cu(I) complexes demonstrated the ability to differentiate between *N*-nitrosamines and a secondary amine and a ppm level limit of detection was determined for **3-Cu**. Studies on structural activity relations using different weakly coordinating anions, solvent and oxidation states of copper were also performed. Weakly coordinating anions unexpectedly influenced the photophysical properties of the binuclear cationic core. $Cu(ClO_4)_2{\cdot}6H_2O$ was demonstrated to oxidize phosphine **5** *in situ* during complexation and gave a different coordination complex **5-Cu-II**, which was more emissive in acetonitrile solution than **5-Cu-ClO$_4$**.

4. Experimental

4.1 General

All reagents were purchased from commercial sources (Sigma-Aldrich, TCI, Strem) and used as received unless stated otherwise. Solvents were degassed by sparging with nitrogen where mentioned. Synthesis of phosphines were performed under inert atmosphere unless stated otherwise. Complexation reactions may be performed either under ambient conditions or inert atmosphere. Anhydrous MeCN was obtained by drying over activated 4 Å molecular sieves. NDMA was synthesized by Robert G. Croy.

NMR spectra were acquired at the MIT Department of Chemistry Instrumentation Facility (DCIF) on Bruker Avance-III HD Nanobay (400 MHz) and Bruker Avance Neo spectrometers (400 and 500 MHz) at ambient temperatures. Referencing was performed during data acquisition using universal chemical shift referencing against the deuterated solvent used. Data in NMR spectra were reported as detailed below: chemical shift (ppm), integration, peak shape (br = broad, s = singlet, d = doublet, t = triplet, m = multiplet, qu = quintet), coupling constant (Hz). EPR spectrum was acquired on a Bruker EMX-Plus spectrometer with an X-band resonator at 4.5 K.

High resolution mass spectra (HRMS) were acquired on a JEOL AccuTOF 4G LC-plus equipped with an ionSense DART (Direct Analysis in Real Time) source for phosphines **1–5**. HRMS for complexes **1-Cu–5-Cu** were obtained on an Agilent 6545 mass spectrometer coupled to an Agilent Infinity 1260 LC system running a Jet Stream electrospray ionization (ESI) source.

UV-visible spectra were obtained on an Agilent Cary 4000 running software version 4.20 (468) using a 1 cm path-length quartz cuvette. Fluorescence measurements were performed at room temperature on a Horiba Jobin Yvon Fluorolog 3 and spectra acquired were corrected for solvent background signals as well as for variances in detector sensitivity for different wavelengths. Excitation measurements were made on the same instrument and the data are only corrected for solvent background signals. Quantum yield measurements were performed on a Horiba Quanta-φ F3029 integrating sphere.

Crystallographic data were collected on a Bruker Photon3 CPAD diffractometer using Mo Kα radiation. Structural solution was obtained using SHELXT-2015 and refinement was performed using SHELXL2018/3. The CIF data of complexes are deposited in the Cambridge Structural Database with CCDC numbers of 2218757, 2218758, 2218759, 2218760, 2218761, 2218762, 2218763, 2218764, 2218765 and 2218766.†

X-ray photoelectron spectroscopy (XPS) measurements were performed on a Thermo Scientific K-Alpha + X-ray photoelectron spectrometer using an Al Kα radiation source.

4.2 Synthesis of diphenylarylphosphines 1–5

4.2.1 Ph$_2$P(2-pyrimidine) (1). This was synthesized using an adapted procedure from literature.[28,68] 2-Chloropyrimidine is a white solid which may be purified from browned commercial samples by extraction with hexanes, filtration to removed undissolved solids and removal of solvent *in vacuo*. Ph_2PH (1 ml, 1.07 g, 5.75 mmol) was added to an oven dried Schlenk flask with a stir bar, placed under nitrogen and diluted with anhydrous THF (4.25 ml). The mixture was placed in a cooling bath (1 : 2 MeOH : H_2O in dry ice) and brought down to −20 °C. *n*-BuLi (1.6 M in hexanes, 3.6 ml, 5.76 mmol) was then added dropwise in 2 batches and stirring continued for 60 min. 2-Chloropyrimidine (656.1 mg, 5.75 mmol) was then added in 4 batches under positive nitrogen flow. The cooling bath was removed and the mixture warmed up to room temperature while stirring over 4 hours. The reaction was quenched with D.I. H_2O (5.8 ml) and extracted with EtOAc (3 × 5 ml). The combined organic layer was dried with brine (7 ml) before being removed *in vacuo* to give the crude product as a yellow solid. Recrystallisation was performed twice (MeOH : DCM = 5 : 1) to give the pure product as white translucent crystals (378 mg, 1.43 mmol, 25% yield). Characterization data matches literature values.

δ_H (400 MHz, $CDCl_3$, ppm): 8.73 (2 H, d, J = 5.0 Hz), 7.61–7.49 (4 H, m), 7.43–7.38 (6 H, m), 7.15 (1 H, d, J = 5.0 Hz).

$\delta_{P\{H\}}$ (162 MHz, $CDCl_3$, ppm): 1.76.

HRMS(DART+): $[C_{16}H_{14}N_2P]^+$ m/z = 265.08811, calcd = 265.08891.

4.2.2 Ph$_2$P(2-quinazoline) (2). This was synthesized using a modified literature procedure for Pd catalyzed coupling.[69] Pd $(OAc)_2$ (1.3937 mg, 0.01 mmol), KOAc (92 mg, 0.93 mmol), 2-chloroquinazoline (107.5 mg, 0.62 mmol) and diphenylphosphine (0.13 ml, 0.74 mmol) were added in that order to an oven dried pressure tube with a plunger valve under a positive flow of nitrogen. Anhydrous dimethylacetamide (DMAc) (0.70 ml) was added and the resulting mixture freeze–pump–thawed four times. During the last cycle, the headspace was evacuated and backfilled with nitrogen thrice before thawing. It was then placed in a pre-heated oil bath at 130 °C (21.5 h). After cooling the reaction to r.t., D.I water (5 ml) was added to the reaction, resulting in the phase separation of an aqueous phase and a red viscous phase stuck to the walls. The aqueous phase was removed before diluting the viscous phase with DCM (7 ml). The organic phase was then washed with water (12 ml) followed by brine (3 ml). It was then dry loaded onto

neutralized silica (treated by Et_3N in hexanes) and eluted with 2 : 1 hexanes : EtOAc and Et_3N (1 vol%) to give the desired product as a pale yellow solid (36.8 mg, 0.12 mmol, 16% yield). The purified product turns increasingly yellow over time under ambient conditions and should be stored under inert atmosphere.

^{31}P NMR of the yellowed material shows the development of a signal likely from the phosphine oxide.

δ_H (400 MHz, $CDCl_3$, ppm): 9.35 (1 H, s), 8.00 (1 H, d, J = 8.6 Hz), 7.91–7.85 (2 H, m), 7.64, (1 H, t, J = 6.9 Hz), 7.63–7.58 (4 H, m), 7.43–7.36 (6 H, m).

$\delta_{P\{H\}}$ (162 MHz, $CDCl_3$, ppm): 1.85.

δ_C (101 MHz, $CDCl_3$, ppm): 172.29, 172.17, 159.45, 159.37, 150.00, 134.76, 134.56, 134.05, 129.13, 128.56, 128.45, 128.37, 127.90, 127.16, 123.18.

HRMS(DART+): $[C_{20}H_{16}N_2P]^+$ m/z = 315.10445, calcd = 315.10456.

4.2.3 Ph_2P(3-isoquinoline) (3). This was synthesized using a modified literature procedure.[23] 3-Chloroisoquinoline (943.8 mg, 5.77 mmol) was placed under N_2 and dissolved in anhydrous THF (1 ml) in an oven dried flask with a stir bar. Separately, $HPPh_2$ (1 ml, 1.07 g, 5.75 mmol) was also put under N_2 before diluting with anhydrous THF (3 ml) and cooled to −20 °C (1 : 2 MeOH : H_2O in dry ice) in an oven fried Schlenk flask with a stir bar. *n*-BuLi (3.6 ml, 1.6 M in hexanes, 5.76 mmol) was added dropwise while stirring to give a deep red solution. Stirring was continued at −20 °C for 10 min after complete addition before removing the cooling bath and stirring for a further 50 min. The 3-chloroisoquinoline solution was then added dropwise and the dark red mixture was stirred overnight (22 h) at r.t. (19 °C). D.I. H_2O (5 ml) was used to quench the reaction. The aqueous layer was extracted once with EtOAc (4 ml) and the combined organic layer was washed with brine (7 ml). The solvent was then removed *in vacuo* to give the crude product as a viscous yellow oil which was further purified *via* column chromatography (hexanes : EtOAc) to give the desired product as a pale-yellow solid (150 mg, 9% yield). Subsequent washing of the solid by minimal cold MeOH removed remaining phosphorus impurities.

Characterization data matches literature values.

δ_H (500 MHz, $CDCl_3$, ppm): 9.35 (1 H, s), 7.98 (1 H, d, J = 8.3 Hz), 7.69–7.61 (3 H, m), 7.48–7.42 (5 H, m), 7.41–7.36 (6 H, m).

$\delta_{P\{H\}}$ (203 MHz, $CDCl_3$, ppm): −4.61.

$\delta_{C\{H\}}$ (126 MHz, $CDCl_3$, ppm): 155.98, 155.93, 152.93, 152.83, 136.44, 136.36, 135.58, 135.55, 134.33, 134.18, 130.63, 129.05, 128.67, 128.61, 127.84, 127.60, 127.51, 126.61, 125.64, 125.51.

HRMS(DART+): $[C_{21}H_{17}NP]^+$ m/z = 314.10884, calcd = 314.10931.

4.2.4 Ph_2P(2-quinoline) (4). This was synthesized using a modified literature procedure.[23] 2-Chloroquinoline should be a white solid which may be purified from browned commercial samples by extracting with hexanes, filtering off the solids and removing the solvent *in vacuo*. Ph_2PH (1 ml, 1.07 g, 5.75 mmol) was placed under nitrogen and diluted with anhydrous THF (2 ml) and cooled to −20 °C (2 : 1 EtOH : H_2O in dry ice) in an oven fried Schlenk flask with a stir bar. *N*-BuLi (3.6 ml, 1.6 M in hexanes, 5.76 mmol) was added dropwise while stirring to give a deep red solution. The cooling bath was removed after the solution was frozen and the mixture allowed to thaw at r.t. (1 h). Additional anhydrous THF (2 ml) was added to help dissolve residual yellow solid. 2-Chloroquinoline (955.8 mg, 5.84 mmol) was then added in small batches. The red solution turned darker before becoming green after 5 min and increasingly cloudy. The mixture was stirred overnight at r.t. (24 h). D.I. H_2O (5 ml) was used to quench the reaction, giving an orange solution phase. The organic layer was isolated and diluted with EtOAc (10 ml) and DCM (10 ml) before filtering off undissolved solids. The filtrate was then washed with brine (5 ml) and dried over anhydrous $MgSO_4$. The solvents were removed *in vacuo* to give the crude product as a viscous yellow oil which was diluted with 1 : 1 (EtOAc : hexane) and filtered over a pad of silica. The purified product was obtained *via* column chromatography (1 : 1 hexane : EtOAc) (317.8 mg, 1.01 mmol, 18% yield) as a pale yellow solid that turns increasingly yellow over time under ambient conditions and should be stored under inert atmosphere.

Characterization data matches literature values.

^{31}P NMR of the yellowed material suggests some oxidation to the phosphine oxide.

δ_H (500 MHz, $CDCl_3$, ppm): 8.18 (1 H, d, J = 8.3 Hz), 8.02 (1 H, d, J = 8.3 Hz), 7.79 (1 H, d, J = 8.1 Hz), 7.73 (1 H, t, J = 6.8 Hz), 7.55 (1 H, t, J = 6.93 Hz), 7.52–7.46 (4 H, m), 7.42–7.36 (6 H, m), 7.23 (1 H, d, J = 8 Hz).

δ_P (203 MHz, $CDCl_3$, ppm): −2.15 (quintet).

$\delta_{C\{H\}}$ (126 MHz, $CDCl_3$, ppm): 164.91, 147.90, 136.37, 136.28, 135.40, 134.31, 134.16, 129.71, 129.69, 129.07, 128.67, 128.61, 127.63, 126.90, 126.84, 124.39.

HRMS(DART+): $[C_{21}H_{17}NP]^+$ m/z = 314.10759, calcd = 314.10931.

4.2.5 Ph_2P(1-isoquinoline) (5). This was synthesized using a modified literature procedure.[23] 1-Chloroisoquinoline (949.7 mg, 5.83 mmol) was dissolved in anhydrous THF (1 ml) in an oven dried flask with a stir bar. Separately, $HPPh_2$ (1 ml, 1.07 g, 5.75 mmol) was diluted with anhydrous THF (3 ml) and cooled to −20 °C (1 : 2 MeOH : H_2O in dry ice) in an oven fried Schlenk flask with a stir bar. *n*-BuLi (4.2 ml, 1.6 M in hexanes, 6.72 mmol) was added dropwise while stirring to give a deep red solution. Stirring was continued at −20 °C after complete addition (15 min) before removing the cooling bath and stirring for a further 1.5 h. The 1-chloroisoquinoline solution was then added dropwise and the resulting dark green mixture was stirred overnight (21 h) at r.t. (19 °C). D.I. H_2O (2.4 ml) was used to quench the reaction, giving a white precipitate which was isolated *via* filtration. It was then washed with H_2O (10 ml) and Et_2O (10 ml) before being dried to give the crude product (1.028 g, 67% yield) which was used for subsequent reactions without further purification.

Characterization data matches literature values.

δ_H (400 MHz, $CDCl_3$, ppm): 8.67–8.63 (1 H, m), 8.61 (1 H, d, J = 7.1 Hz), 7.84 (1 H, d, J = 8.2 Hz), 7.67 (1 H, t, J = 7.1 Hz),

7.60 (1 H, d, J = 5.6 Hz), 7.53 (1 H, t, J = 7.1 Hz), 7.47–7.39 (4 H, m), 7.38–7.31 (6 H, m).

$\delta_{P\{H\}}$ (162 MHz, $CDCl_3$, ppm): −8.29.

$\delta_{C\{H\}}$ (101 MHz, $CDCl_3$, ppm): 163.73, 163.63, 143.20, 135.41, 134.60, 134.40, 132.19, 131.90, 130.08, 128.92, 128.44, 128.36, 127.35, 127.33, 127.19, 127.05, 126.82, 120.43.

HRMS(DART+): $[C_{21}H_{17}NP]^+$ m/z = 314.10800, calcd = 314.10931.

4.2.6 Synthesis of Ph_2P(1-isoquinoline) phosphine oxide (5-O). This was synthesized following a modified literature procedure.[70,71] Ph_2P(1-isoquinoline) (20 mg, 0.06 mmol) was dissolved in EtOAc (3 ml) and H_2O_2 (27% w/w aqueous solution, 100 μl) added. The mixture was stirred at r.t. (2 h) after which the reaction was complete by TLC. The reaction mixture was dried over Na_2SO_4 before being filtered over a pad of silica. The solvent was removed to give the desired product (15.5 mg, 0.05 mmol, 83% yield).

Characterization data matches literature values.

δ_H (400 MHz, $CDCl_3$, ppm): 9.47 (1 H, d, J = 8.5 Hz), 8.65 (1 H, d, J = 5.5 Hz), 7.98–7.84 (2 H, m), 7.79–7.70 (2 H, m), 7.66 (1 H, t, J = 7.7 Hz), 7.61–7.42 (7 H, m).

$\delta_{P\{H\}}$ (162 MHz, $CDCl_3$, ppm): 28.5.

HRMS(ESI+) $[C_{21}H_{17}NPO]^+$ m/z = 330.1047, calcd = 330.1048.

4.3 Synthesis of tetrakisacetonitrilecopper(I) perchlorate ([Cu(MeCN)$_4$]ClO$_4$)

CAUTION: Perchlorate compounds are strong oxidizers and may pose explosion and fire hazards. Ensure proper protective equipment is worn and exercise care when working with these materials! This was synthesized using a literature procedure.[72,73] Cu_2O (298.6 mg) was suspended in acetonitrile (9 ml) and 70 wt% perchloric acid solution (0.34 ml) added to the suspension. The mixture was stirred at r.t (2 h), during which the black solids dissolved and gave a white precipitate. Additional MeCN (20 ml) was added to dissolve the white solids before filtering off any remaining insoluble material. The solvent was removed *in vacuo* to give white crystals and dried under vacuum (3 h). They were then stored under nitrogen (2.8 g). The solids gain a blue hue over time at room temperature and should therefore ideally be prepared and used fresh as required.

4.4 Complexation of Cu with phosphines 1–5

4.4.1 Synthesis of 1-Cu. This was synthesized following a modified literature procedure.[28] $[Cu(MeCN)_4]PF_6$ (94.2 mg, 0.25 mol, 1 equiv.) was added to an oven fried schlenk flask with a stir bar, dissolved in anhydrous MeCN (2.55 ml) and placed under nitrogen, giving a clear solution. Ph_2P(2-pyrimidine) (103.2 mg, 0.38 mol, 1.5 equiv.) was then added and stirring continued at room temperature overnight. The resulting clear solution was added dropwise to Et_2O (20 ml) and white precipitate (100 mg, 0.08 mmol, 32% yield) isolated *via* filtration over a polypropylene membrane (0.6 μm). A solution of 2 : 1 MeOH : DCM (5 ml) was added to the crude material before centrifuging the mixture and isolating the supernatant. The supernatant was slowly evaporated overnight to give crystals that fluoresce green.

δ_H (500 MHz, CD_3OD, ppm): 9.10 (br s), 7.74 (br s), 7.44 (t, J = 7.3 Hz), 7.28 (t, J = 8.0 Hz), 7.16 (br s).

δ_P (203 MHz, CD_3OD, ppm): 9.84 (br s), −144.60 (quintet, J = 707 Hz, PF_6^-).

δ_F (471 MHz, CD_3OD, ppm): −74.74 (d, J = 707.4 Hz, PF_6^-).

HRMS(ESI+): $[C_{48}H_{39}CuN_6P_3]^+$ m/z = 855.1743, calcd = 855.1745. $[C_{32}H_{26}CuN_4P_2]^+$ m/z = 591.0922, calcd = 591.0929. $[C_{16}H_{13}CuN_2P]^+$ m/z = 327.0109, calcd = 327.0112.

4.4.2 Synthesis of 2-Cu‡. This was synthesized following a modified literature procedure.[28] Ph_2P(2-quinazoline) (123 mg, 0.4 mmol) and $[Cu(MeCN)_4]PF_6$ (97 mg, 0.26 mmol) were added to 1 dram vial. MeCN (1 ml) was added and the resulting yellow solution was stirred at r.t. (21 h), during which some product may form and give a yellow suspension. Further Et_2O may be added to precipitate more product. The precipitated solids were isolated *via* filtration and washed with Et_2O (5 ml) to give the crude product as a yellow powder that fluorescence orange (8.1 mg, 5.8 μmol, 11% yield). It may be further purified by redissolving it in minimal MeCN and precipitating with Et_2O twice.

δ_H (400 MHz, $CDCl_3$, ppm) 9.94 (br s), 8.29 (br s), 8.09 (t, J = 7.7 Hz), 7.94 (br s), 7.87 (t, J = 7.1 Hz), 7.16 (br s), 7.09 (br s).

$\delta_{P\{H\}}$ (162 MHz, $CDCl_3$, ppm): 10.68 (br s), −144.03 (sept, PF_6^-).

δ_C (101 MHz, $CDCl_3$, ppm) 161.44, 149.10, 137.14, 133.14, 131.02, 130.80, 128.89, 128.22.

HRMS(ESI+): $[C_2H_3CuN]^+$ m/z = 103.9554, calcd = 103.9562. $[C_{60}H_{45}CuN_6P_3]^+$ m/z = 1005.2242, calcd = 1005.2215. $[C_{40}H_{30}CuN_4P_2]^+$ m/z = 691.1262, calcd = 691.1242. $[C_{22}H_{18}CuN_3P]^+$ m/z = 418.0545, calcd = 418.0534. $[C_{20}H_{15}CuN_2P]^+$ m/z = 377.0271, calcd = 377.0269.

4.4.3 Synthesis of 3-Cu‡. This was synthesized following a modified literature procedure.[28] $[Cu(MeCN)_4]PF_6$ (54 mg, 0.15 mmol) and PPh_2(3-isoquinoline) (69 mg, 0.22 mmol) were added to an oven dried Schlenk flask with a stir bar and placed under N_2. Anhydrous MeCN (1.6 ml) was added to the solids and the resulting mixture was stirred at room temperature (23 h) to give a yellow solution containing a white suspension. The mixture was filtered through a syringe filter (0.2 μm) to give a clear yellow solution. The filtered solution was then added to Et_2O (20 ml) and left to stand without stirring (1 h), during which it separated into three layers. From top to bottom: white cloudy suspension, clear yellow solution and white crystals. The product was filtered off as white crystals (34.1 mg, 0.02 mmol, 13% yield).

δ_H (500 MHz, $CDCl_3$, ppm): 10.14 (br s), 9.75 (br s), 8.50 (br s), 8.25 (br s), 7.82 (br s), 7.58 (br s), 7.09 (br s).

$\delta_{P\{H\}}$ (203 MHz, $CDCl_3$, ppm): 2.56 (br s), −144.00 (quintet, PF_6^-).

$\delta_{C\{H\}}$ (126 MHz, $CDCl_3$, ppm) 155.78, 134.75, 132.89, 130.73, 129.04, 126.50.

‡ Please refer to Experimental details section in ESI for more details.

HRMS(ESI+): $[C_2H_3CuN]^+$ m/z = 103.9554, calcd = 103.9562. $[C_{63}H_{48}CuN_3P_3]^+$ m/z = 1002.2375, calcd = 1002.2357. $[C_{42}H_{32}CuN_2P_2]^+$ m/z = 689.1352, calcd = 689.1337. $[C_{23}H_{19}CuN_2P]^+$ m/z = 417.0590, calcd = 417.0582. $[C_{21}H_{16}CuNP]^+$ m/z = 376.0321, calcd = 376.0316.

4.4.4 Synthesis of 4-Cu‡. This was synthesized following a modified literature procedure.[28] Ph_2P(2-quinoline) (99.7 mg, 0.32 mmol) and $[Cu(MeCN)_4]PF_6$ (76.3 mg, 0.21 mmol) were placed under nitrogen and dissolved in anhydrous MeCN (2 ml). The resulting solution was stirred at r.t. (18 h) before removing insoluble solids using a syringe filter (0.2 μm) to give a clear yellow solution. Et_2O (20 ml) was added to the solution to precipitate the product as a yellow powder with a lime green fluorescence (68 mg, 0.05 mmol, 24% yield).

δ_H (500 MHz, CD_3CN, ppm) 7.91 (br s), 7.80 (t, J = 8.8 Hz), 7.72 (t, J = 7.64 Hz), 7.61 (t, J = 8.0 Hz), 7.54 (t, J = 7.9 Hz), 7.50 (t, J = 7.7 (Hz)), 7.40 (t, J = 7.3 Hz).

$\delta_{P\{H\}}$ (203 MHz, CD_3CN, ppm): 0.26 (br s), −144.63 (sept, PF_6^-).

δ_C (126 MHz, CD_3CN, ppm): 135.18, 135.06, 131.44, 131.20, 129.81, 129.74, 129.01, 128.58, 128.06, 124.95, 124.77.

HRMS(ESI+): $[C_2H_3CuN]^+$ m/z = 103.9554, calcd = 103.9562. $[C_{63}H_{48}CuN_3P_3]^+$ m/z = 1002.2385, calcd = 1002.2357. $[C_{42}H_{32}CuN_2P_2]^+$ m/z = 689.1359, calcd = 689.1337. $[C_{23}H_{19}CuN_2P]^+$ m/z = 417.0586, calcd = 417.0582. $[C_{21}H_{16}CuNP]^+$ m/z = 376.0317, calcd = 376.0316.

4.4.5 Synthesis of 5-Cu-PF_6. This was synthesized following a modified literature procedure.[28] $[Cu(MeCN)_4]PF_6$ (76.4 mg, 0.21 mmol) was dissolved in anhydrous MeCN (2 ml) in an oven dried flask with a stir bar. Separately, Ph_2P(1-isoquinoline) (99.8 mg, 0.32 mmol) was added to an oven dried Schlenk flask with a stir bar. The copper(I) solution was added dropwise to the phosphine while stirring and the resulting pale yellow solution stirred at r.t. (21 h). It was then added dropwise to rapidly stirred Et_2O (48 ml) to give a yellow precipitate. After complete addition, additional Et_2O (20 ml) was added and stirring continued (15 min). The product was isolated as a yellow powder that fluoresces red *via* vacuum filtration (69.9 mg, 0.05 mmol, 24% yield).

δ_H (500 MHz, $CDCl_3$, ppm): 9.42 (br s), 9.27 (br s), 8.41 (br s), 8.02 (br s), 7.68 (br s), 7.37 (br s), 7.16 (br s), 6.73.

δ_F (471 MHz, $CDCl_3$, ppm): −73 (d, PF_6^-).

$\delta_{P\{H\}}$ (203 MHz, $CDCl_3$, ppm): 14.60 (2 P, br s), 7.79 (1 P, br s), −144.04 (2 P, quintet, PF_6^-).

HRMS(ESI+): $[C_2H_3CuN]^+$ m/z = 103.9554, calcd = 103.9562. $[C_{63}H_{48}CuN_3P_3]^+$ m/z = 1002.2332, calcd = 1002.2357. $[C_{42}H_{32}CuN_2P_2]^+$ m/z = 689.1354, calcd = 689.1337. $[C_{23}H_{19}CuN_2P]^+$ m/z = 417.0585, calcd = 417.0582. $[C_{21}H_{16}CuNP]^+$ m/z = 376.0316, calcd = 376.0316.

4.4.6 Synthesis of 5-Cu-ClO_4. This was synthesized following a modified literature procedure.[28] $[Cu(MeCN)_4](ClO_4)$ (123.4 mg, 0.38 mmol) was suspended in MeCN (5 ml). Ph_2P (1-isoquinoline) (170.9 mg, 0.55 mmol) was added to the cloudy suspension and stirred at r.t. (4 h) to give a yellow solution. Et_2O (55 ml) was added to the yellow solution and the mixture cooled in a fridge (1 h). The precipitate was isolated *via* filtration and washed with Et_2O (15 ml). The product was isolated as a yellow powder and dried overnight *in vacuo* (201.3 mg, 0.15 mmol, 40% yield).

δ_H (500 MHz, $CDCl_3$, ppm): 9.46 (1 H d, J = 4.1 Hz), 8.42 (1 H, br s), 8.00 (1 H, d, J = 8.0 Hz), 7.66 (1 H, t, J = 6.9 Hz), 7.39 (1 H, d, J = 8.8 Hz), 7.18 7.26–6.9 (9 H, br d).

δ_P (203 MHz, $CDCl_3$, ppm): 13.41 (2 P, br s), 7.10 (1 P, br s).

HRMS(ESI+): $[C_2H_3CuN]^+$ m/z = 103.9554, calcd = 103.9562. $[C_{63}H_{48}CuN_3P_3]^+$ m/z = 1002.2305, calcd = 1002.2357. $[C_{42}H_{32}CuN_2P_2]^+$ m/z = 689.1333, calcd = 689.1337. $[C_{23}H_{19}CuN_2P]^+$ m/z = 417.0586, calcd = 417.0582. $[C_{21}H_{16}CuNP]^+$ m/z = 376.0318, calcd = 376.0316.

4.4.7 Adding NDMA to 5-Cu-ClO_4. NDMA was added to a $CDCl_3$ solution containing **5-Cu-ClO_4** before acquiring the spectra.

δ_H (500 MHz, $CDCl_3$, ppm): 9.42 (1 H, d, J = 5.5 Hz), 8.42 (br s), 8.00 (1 H, d, J = 8.2 Hz), 7.65 (1 H, t, J = 7.3 Hz), 7.38 (1 H, d, J = 8.1 Hz), 7.25–7.69 (2 H, br d), 3.82 (10 H, s, NDMA), 3.10 (10 H, s, NDMA).

δ_P (203 MHz, $CDCl_3$, ppm): 13.34 (2 P, br s), 6.72 (1 P, br s).

4.4.8 Synthesis of 5-Cu-II from 5. This was synthesized following a modified literature procedure for complexation with Cu(I).[28] $Cu(ClO_4)_2{\cdot}6H_2O$ (71.1 mg, 0.19 mmol) and Ph_2P(1-isoquinoline) (92.4 mg, 0.30 mmol) were dissolved in MeCN (2 ml) and stirred at r.t. under air (2.5 h). A dark green solution initially forms and turns light green over 1 h. The solvent was removed *in vacuo* to yield a light green solid as the crude product. The purified product was obtained by recrystallizing from MeCN–Et_2O (27 mg, 0.03 mmol, 20% yield).

δ_H (500 MHz, CD_3CN, ppm): 11.47 (br s), 10.39 (br s), 8.84 (br s), 8.59 (d, J = 8.7 Hz), 8.38(s), 8.30 (d, J = 8.5 Hz), 8.17 (t, J = 7.9 Hz), 7.90 (t, J = 7.9 Hz), 7.65 (t, J = 7.1 Hz), 7.60–7.50 (m), 7.24 (br s), 6.38 (br s), 5.90 (br s).

δ_P (203 MHz, CD_3CN, ppm): −6.88 (s).

HRMS(ESI+): $[C_{42}H_{32}CuN_2O_2P_2]^+$ m/z = 721.1245, calcd = 721.1235. $[C_{21}H_{16}CuNOP]^+$ m/z = 392.0266, calcd = 392.0266. $[C_{21}H_{17}NOP]^+$ m/z = 330.1045, calcd = 330.0970. $[C_{23}H_{19}N_2OP]^+$ m/z = 433.0535, calcd = 433.0531.

4.4.9 Synthesis of 5-Cu-II from 5-O. Ph_2P(1-isoquinoline) oxide **5-O** (13.2 mg, 0.04 mmol) was suspended in MeCN (1.2 ml). $CuClO_4{\cdot}6H_2O$ (7.5 mg, 0.02 mmol) was then added to the suspension while stirring. Immediately after addition of Cu(II), the solution turned light blue and gradually darker blue. DCM (approx. 2 ml) was added to help dissolve phosphine oxide above the MeCN solvent line. The solution was stirred at room temperature overnight (19 h). The solvent was then removed *in vacuo* to give a product as a blue solid which was used for further characterisation (14.4 mg, 0.016 mmol, 78% yield).

δ_H (500 MHz, CD_3CN, ppm): 10.7 (br s), 9.87 (br s), 8.55 (br s), 7.64 (br s), 6.68 (br s), 6.23 (br s).

δ_P (203 MHz, CD_3CN, ppm): no signal.

HRMS(ESI+): $[C_{42}H_{32}CuN_2O_2P_2]^+$ m/z = 721.1241, calcd = 721.1235. $[C_{21}H_{16}CuNOP]^+$ m/z = 392.0268, calcd = 392.0266.

4.4.10 Adding NDMA to 5-Cu-II. NDMA was added to a $CDCl_3$ solution containing **5-Cu-II** before acquiring the spectra.

δ_H (500 MHz, CD_3CN, ppm): 11.31 (br s), 10.29 (br s), 8.78 (br s), 8.60 (d, J = 9 Hz), 8.37 (m), 8.30 (d, J = 8.3 Hz), 8.18 (t, J = 7.8 Hz), 7.90 (t, J = 7.7 Hz), 7.61–7.61 (m), 7.60–7.49 (m), 7.31 (br s), 6.45 (br s), 5.97 (br s), 3.75 (s, NDMA), 3.03 (s, NDMA).

Author contributions

Haosheng Feng: conceptualization, investigation, writing – original draft and writing – review & editing. Shao-Xiong Lennon Luo: writing – review & editing and XPS characterization. Robert G. Croy and John M. Essigmann: resources – synthesized and provided NDMA used in the study and writing – review & editing. Timothy M. Swager: supervision, conceptualization, funding acquisition and writing – review & editing.

Conflicts of interest

There are no conflicts to declare.

Acknowledgements

The authors would like to thank the National Institute of Environmental Health Sciences Superfund Basic Research Program, National Institutes of Health (P42 ES027707), as well as the National Cancer Institute (R01 CA80024) for funding. Dr Peter Mueller's services in acquiring, solving and refining crystallographic data is also greatly appreciated. XPS experiments were performed at the Harvard University Center for Nanoscale Systems (CNS); a member of the National Nanotechnology Coordinated Infrastructure Network (NNCI), which is supported by the National Science Foundation under NSF award no. ECCS-2025158.

References

1 J. C. Beard and T. M. Swager, *J. Org. Chem.*, 2021, **86**, 2037–2057.
2 J. E. Kay, J. J. Corrigan, A. L. Armijo, I. S. Nazari, I. N. Kohale, D. K. Torous, S. L. Avlasevich, R. G. Croy, D. N. Wadduwage, S. E. Carrasco, S. D. Dertinger, F. M. White, J. M. Essigmann, L. D. Samson and B. P. Engelward, *Cell Rep.*, 2021, **34**, 108864.
3 A. E. Pegg and G. Hui, *Biochem. J.*, 1978, **173**, 739–748.
4 J. A. Swenberg, D. G. Hoel and P. N. Magee, *Cancer Res.*, 1991, **51**, 6409–6414.
5 M. Krauss, P. Longrée, F. Dorusch, C. Ort and J. Hollender, *Water Res.*, 2009, **43**, 4381–4391.
6 J. M. Fajen, G. A. Carson, D. P. Rounbehler, T. Y. Fan, R. Vita, U. E. Goff, M. H. Wolf, G. S. Edwards, D. H. Fine, V. Reinhold and K. Biemann, *Science*, 1979, **205**, 1262–1264.
7 K. Kosaka, M. Asami, K. Ohkubo, T. Iwamoto, Y. Tanaka, H. Koshino, S. Echigo and M. Akiba, *Environ. Sci. Technol.*, 2014, **48**, 11243–11250.
8 H. S. Lee, *Food Addit. Contam., Part A*, 2019, **36**, 1491–1500.
9 N. P. Sen, J. R. Iyengar, W. F. Miles and T. Panalaks, *IARC Sci. Publ.*, 1976, 333–342 (IARC: International Agency for Research on Cancer).
10 S. Schmidtsdorff, J. Neumann, A. H. Schmidt and M. K. Parr, *Arch. Pharm.*, 2022, **355**, 2100435.
11 W. A. Mitch, J. O. Sharp, R. R. Trussell, R. L. Valentine, L. Alvarez-Cohen and D. L. Sedlak, *Environ. Eng. Sci.*, 2003, **20**, 389–404.
12 J. Bridgeman, M. Bieroza and A. Baker, *Rev. Environ. Sci. Biotechnol.*, 2011, **10**, 277.
13 K. A. Emhoff, L. Balaraman, A. M. H. Salem, K. I. Mudarmah and W. C. Boyd, *Coord. Chem. Rev.*, 2019, **396**, 124–140.
14 G.-B. Yi, M. A. Khan and G. B. Richter-Addo, *J. Am. Chem. Soc.*, 1995, **117**, 7850–7851.
15 L. Chen, G.-B. Yi, L.-S. Wang, U. R. Dharmawardana, A. C. Dart, M. A. Khan and G. B. Richter-Addo, *Inorg. Chem.*, 1998, **37**, 4677–4688.
16 N. Xu, L. E. Goodrich, N. Lehnert, D. R. Powell and G. B. Richter-Addo, *Inorg. Chem.*, 2010, **49**, 4405–4419.
17 M. G. White, R. J. Colton, T. H. Lee and J. W. Rabalais, *Chem. Phys.*, 1975, **8**, 391–398.
18 Z. Abedin-Siddique, T. Ohno, K. Nozaki and T. Tsubomura, *Inorg. Chem.*, 2004, **43**, 663–673.
19 A. R. G. Smith, P. L. Burn and B. J. Powell, *ChemPhysChem*, 2011, **12**, 2429–2438.
20 M. Klein, N. Rau, M. Wende, J. Sundermeyer, G. Cheng, C.-M. Che, A. Schinabeck and H. Yersin, *Chem. Mater.*, 2020, **32**, 10365–10382.
21 M. Osawa, I. Kawata, R. Ishii, S. Igawa, M. Hashimoto and M. Hoshino, *J. Mater. Chem. C*, 2013, **1**, 4375–4383.
22 P. C. Ford, E. Cariati and J. Bourassa, *Chem. Rev.*, 1999, **99**, 3625–3648.
23 D. M. Zink, M. Bächle, T. Baumann, M. Nieger, M. Kühn, C. Wang, W. Klopper, U. Monkowius, T. Hofbeck, H. Yersin and S. Bräse, *Inorg. Chem.*, 2013, **52**, 2292–2305.
24 C. E. McCusker and F. N. Castellano, *Inorg. Chem.*, 2013, **52**, 8114–8120.
25 Y. Zhang, M. Schulz, M. Wächtler, M. Karnahl and B. Dietzek, *Coord. Chem. Rev.*, 2018, **356**, 127–146.
26 K. Tsuge, Y. Chishina, H. Hashiguchi, Y. Sasaki, M. Kato, S. Ishizaka and N. Kitamura, *Coord. Chem. Rev.*, 2016, **306**, 636–651.
27 E. Cariati, E. Lucenti, C. Botta, U. Giovanella, D. Marinotto and S. Righetto, *Coord. Chem. Rev.*, 2016, **306**, 566–614.
28 A. V. Artem'ev, M. P. Davydova, A. S. Berezin, M. R. Ryzhikov and D. G. Samsonenko, *Inorg. Chem.*, 2020, **59**, 10699–10706.
29 E. Hobbollahi, M. Himmelsbach, M. List and U. Monkowius, *Inorg. Chem. Commun.*, 2016, **71**, 105–108.
30 H. Ohara, T. Ogawa, M. Yoshida, A. Kobayashi and M. Kato, *Dalton Trans.*, 2017, **46**, 3755–3760.

31 T. Hasegawa, A. Kobayashi, H. Ohara, M. Yoshida and M. Kato, *Inorg. Chem.*, 2017, **56**, 4928–4936.
32 U. Monkowius, M. Zabel, M. Fleck and H. Yersin, *Z. Naturforsch., B: J. Chem. Sci.*, 2009, **64**, 1513–1524.
33 Y.-J. Li, Z.-Y. Deng, X.-F. Xu, H.-B. Wu, Z.-X. Cao and Q.-M. Wang, *Chem. Commun.*, 2011, **47**, 9179–9181.
34 B. Krebs and J. Mandt, *Chem. Ber.*, 1975, **108**, 1130–1137.
35 M. Rahm, R. Hoffmann and N. W. Ashcroft, *Chem. – Eur. J.*, 2016, **22**, 14625–14632.
36 P. Pyykkö, *J. Phys. Chem. A*, 2015, **119**, 2326–2337.
37 S.-X. L. Luo, R. Y. Liu, S. Lee and T. M. Swager, *J. Am. Chem. Soc.*, 2021, **143**, 10441–10453.
38 T. S. A. Hor, H. S. O. Chan, K.-L. Tan, L.-T. Phang, Y. K. Yan, L.-K. Liu and Y.-S. Wen, *Polyhedron*, 1991, **10**, 2437–2450.
39 C. Battistoni, G. Mattogno, E. Paparazzo and L. Naldini, *Inorg. Chim. Acta*, 1985, **102**, 1–3.
40 B. H. Aw, K. K. Looh, H. S. O. Chan, K. L. Tan and T. S. A. Hor, *J. Chem. Soc., Dalton Trans.*, 1994, 3177–3182.
41 M. C. Biesinger, L. W. M. Lau, A. R. Gerson and R. St. C. Smart, *Appl. Surf. Sci.*, 2010, **257**, 887–898.
42 R. G. Pearson, *J. Chem. Educ.*, 1968, **45**, 581.
43 R. G. Pearson, *J. Chem. Educ.*, 1968, **45**, 643.
44 E. Lastra, M. P. Gamasa, J. Gimeno, M. Lanfranchi and A. Tiripicchio, *J. Chem. Soc., Dalton Trans.*, 1989, 1499–1506.
45 N. P. Rath, E. M. Holt and K. Tanimura, *Inorg. Chem.*, 1985, **24**, 3934–3938.
46 J. R. Black, W. Levason and M. Webster, *Acta Crystallogr., Sect. C: Cryst. Struct. Commun.*, 1995, **51**, 623–625.
47 M. M. Roessler and E. Salvadori, *Chem. Soc. Rev.*, 2018, **47**, 2534–2553.
48 G. Pilloni, G. Valle, C. Corvaja, B. Longato and B. Corain, *Inorg. Chem.*, 1995, **34**, 5910–5918.
49 M. B. Inoue, E. F. Velazquez and M. Inoue, *Synth. Met.*, 1988, **24**, 223–229.
50 B. J. Brennan, M. J. Kenney, P. A. Liddell, B. R. Cherry, J. Li, A. L. Moore, T. A. Moore and D. Gust, *Chem. Commun.*, 2011, **47**, 10034–10036.
51 N. K. Shee, S. G. Patra, M. G. B. Drew and D. Datta, *J. Coord. Chem.*, 2016, **69**, 3677–3691.
52 K. R. Trigulova, A. V. Shamsieva, R. R. Fayzullin, A. I. Kasimov, E. I. Musina and A. A. Karasik, *Phosphorus, Sulfur Silicon Relat. Elem.*, 2022, **197**, 620–624.
53 K. R. Trigulova, A. V. Shamsieva, R. R. Faizullin, P. Lönnecke, E. Hey-Hawkins, A. D. Voloshina, E. I. Musina and A. A. Karasik, *Russ. J. Coord. Chem.*, 2020, **46**, 600–607.
54 Q. Zhang, T. Komino, S. Huang, S. Matsunami, K. Goushi and C. Adachi, *Adv. Funct. Mater.*, 2012, **22**, 2327–2336.
55 A. K. I. Gushurst, D. R. McMillin, C. O. Dietrich-Buchecker and J. P. Sauvage, *Inorg. Chem.*, 1989, **28**, 4070–4072.
56 D. G. Cuttell, S.-M. Kuang, P. E. Fanwick, D. R. McMillin and R. A. Walton, *J. Am. Chem. Soc.*, 2002, **124**, 6–7.
57 S. P. Srinivas and R. Mutharasan, *Biotechnol. Bioeng.*, 1987, **30**, 769–774.
58 G. Van der Zwan and J. T. Hynes, *J. Phys. Chem.*, 1985, **89**, 4181–4188.
59 H. Yang, G. Ran, J. Yan, H. Zhang and X. Hu, *Lumin. J. Biol. Chem. Lumin.*, 2018, **33**, 349–355.
60 P. Das and S. K. Mandal, *J. Mater. Chem. C*, 2018, **6**, 3288–3297.
61 J. Brunner and R. Kraemer, *J. Am. Chem. Soc.*, 2004, **126**, 13626–13627.
62 W. Zou, K. Le and M. L. Zastrow, *ChemBioChem*, 2020, **21**, 1356–1363.
63 M. Oggianu, C. Figus, S. Ashoka-Sahadevan, N. Monni, D. Marongiu, M. Saba, A. Mura, G. Bongiovanni, C. Caltagirone, V. Lippolis, C. Cannas, E. Cadoni, M. L. Mercuri and F. Quochi, *RSC Adv.*, 2021, **11**, 15557–15564.
64 F. Liu, K. L. Cunningham, W. Uphues, G. W. Fink, J. Schmolt and D. R. McMillin, *Inorg. Chem.*, 1995, **34**, 2015–2018.
65 K. L. Cunningham, K. M. McNett, R. A. Pierce, K. A. Davis, H. H. Harris, D. M. Falck and D. R. McMillin, *Inorg. Chem.*, 1997, **36**, 608–613.
66 A. Harriman, *J. Chem. Soc., Faraday Trans. 1*, 1981, **77**, 369–377.
67 M. Barwiolek, E. Szlyk, T. M. Muzioł and T. Lis, *Dalton Trans.*, 2011, **40**, 11012–11022.
68 M. T. Reetz, R. Demuth and R. Goddard, *Tetrahedron Lett.*, 1998, **39**, 7089–7092.
69 R. Gramage-Doria, J. Hessels, S. H. A. M. Leenders, O. Tröppner, M. Dürr, I. Ivanović-Burmazović and J. N. H. Reek, *Angew. Chem., Int. Ed.*, 2014, **53**, 13380–13384.
70 J. H. Walton and H. A. Lewis, *J. Am. Chem. Soc.*, 1916, **38**, 633–638.
71 C. R. Hilliard, N. Bhuvanesh, J. A. Gladysz and J. Blümel, *Dalton Trans.*, 2012, **41**, 1742–1754.
72 P. Hemmerich and C. Sigwart, *Experientia*, 1963, **19**, 488–489.
73 E. J. Parish, H. Qin, B. H. Lipshutz and C.-T. Lee, *in Encyclopedia of Reagents for Organic Synthesis*, John Wiley & Sons, Ltd, 2007.